

Search for dark photons from neutral meson decays in p+p and d+Au collisions at $\sqrt{s_{NN}}=200$ GeV

(PHENIX Collaboration) Adare, A.; ...; Makek, Mihael; ...; Zolin, L.

Source / Izvornik: **Physical Review C - Nuclear Physics, 2015, 91**

Journal article, Published version

Rad u časopisu, Objavljena verzija rada (izdavačev PDF)

<https://doi.org/10.1103/PhysRevC.91.031901>

Permanent link / Trajna poveznica: <https://um.nsk.hr/um:nbn:hr:217:418142>

Rights / Prava: [In copyright](#)/[Zaštićeno autorskim pravom.](#)

Download date / Datum preuzimanja: **2025-02-05**



Repository / Repozitorij:

[Repository of the Faculty of Science - University of Zagreb](#)



Search for dark photons from neutral meson decays in $p + p$ and $d + \text{Au}$ collisions at $\sqrt{s_{NN}} = 200 \text{ GeV}$

A. Adare,¹⁴ S. Afanasiev,³³ C. Aidala,^{42,46,47} N. N. Ajitanand,⁶⁶ Y. Akiba,^{60,61} R. Akimoto,¹³ H. Al-Bataineh,⁵⁴ H. Al-Ta'ani,⁵⁴ J. Alexander,⁶⁶ M. Alfred,²⁶ K. R. Andrews,¹ A. Angerami,¹⁵ K. Aoki,^{38,60} N. Apadula,^{31,67} L. Aphecetche,⁶⁸ E. Appelt,⁷² Y. Aramaki,^{13,60} R. Armendariz,⁹ J. Asai,⁶⁰ H. Asano,^{38,60} E. C. Aschenauer,⁸ E. T. Atomssa,^{39,67} R. Averbeck,⁶⁷ T. C. Awes,⁵⁶ B. Azmoun,⁸ V. Babintsev,²⁷ M. Bai,⁷ G. Baksay,²¹ L. Baksay,²¹ A. Baldissieri,¹⁷ N. S. Bandara,⁴⁶ B. Bannier,⁶⁷ K. N. Barish,⁹ P. D. Barnes,^{42,*} B. Bassalleck,⁵³ A. T. Basye,¹ S. Bathe,^{6,9,61} S. Batsouli,⁵⁶ V. Baublis,⁵⁹ C. Baumann,⁴⁸ A. Bazilevsky,⁸ M. Beaumier,⁹ S. Beckman,¹⁴ S. Belikov,^{8,*} R. Belmont,^{47,72} J. Ben-Benjamin,⁴⁹ R. Bennett,⁶⁷ A. Berdnikov,⁶³ Y. Berdnikov,⁶³ J. H. Bhom,⁷⁶ A. A. Bickley,¹⁴ D. Black,⁹ D. S. Blau,³⁷ J. G. Boissevain,⁴² J. S. Bok,^{54,76} H. Borel,¹⁷ K. Boyle,^{61,67} M. L. Brooks,⁴² D. Broxmeyer,⁴⁹ J. Bryslawskij,⁶ H. Buesching,⁸ V. Bumazhnov,²⁷ G. Bunce,^{8,61} S. Butsyk,⁴² C. M. Camacho,⁴² S. Campbell,^{31,67} A. Caringi,⁴⁹ P. Castera,⁶⁷ B. S. Chang,⁷⁶ W. C. Chang,² J.-L. Charvet,¹⁷ C.-H. Chen,^{61,67} S. Chernichenko,²⁷ C. Y. Chi,¹⁵ M. Chiu,^{8,28} I. J. Choi,^{28,76} J. B. Choi,¹¹ R. K. Choudhury,⁵ P. Christiansen,⁴⁴ T. Chujo,⁷¹ P. Chung,⁶⁶ A. Churny,⁹ O. Chvala,⁹ V. Cianciolo,⁵⁶ Z. Citron,^{67,74} B. A. Cole,¹⁵ Z. Conesa del Valle,³⁹ M. Connors,⁶⁷ P. Constantin,⁴² M. Csanád,¹⁹ T. Csörgő,⁷⁵ T. Dahms,⁶⁷ S. Dairaku,^{38,60} I. Danchev,⁷² K. Das,²² A. Datta,^{46,53} M. S. Daugherty,¹ G. David,⁸ M. K. Dayananda,²³ K. DeBlasio,⁵³ K. Dehmelt,⁶⁷ A. Denisov,²⁷ D. d'Enterria,³⁹ A. Deshpande,^{61,67} E. J. Desmond,⁸ K. V. Dharmawardane,⁵⁴ O. Dietzsch,⁶⁴ L. Ding,³¹ A. Dion,^{31,67} J. H. Do,⁷⁶ M. Donadelli,⁶⁴ O. Drapier,³⁹ A. Drees,⁶⁷ K. A. Drees,⁷ A. K. Dubey,⁷⁴ J. M. Durham,^{42,67} A. Durum,²⁷ D. Dutta,⁵ V. Dzhordzhadze,⁹ L. D'Orazio,⁴⁵ S. Edwards,²² Y. V. Efremenko,⁵⁶ F. Ellinghaus,¹⁴ T. Engelmores,¹⁵ A. Enokizono,^{41,56,60,62} H. En'yo,^{60,61} S. Esumi,⁷¹ K. O. Eyster,⁹ B. Fadem,⁴⁹ N. Feege,⁶⁷ D. E. Fields,^{53,61} M. Finger,¹⁰ M. Finger, Jr.,¹⁰ F. Fleuret,³⁹ S. L. Fokin,³⁷ Z. Fraenkel,^{74,*} J. E. Frantz,^{55,67} A. Franz,⁸ A. D. Frawley,²² K. Fujiwara,⁶⁰ Y. Fukao,^{38,60} T. Fusayasu,⁵¹ C. Gal,⁶⁷ P. Gallus,¹⁶ P. Garg,⁴ I. Garishvili,⁶⁹ H. Ge,⁶⁷ F. Giordano,²⁸ A. Glenn,^{14,41} H. Gong,⁶⁷ X. Gong,⁶⁶ M. Gonin,³⁹ J. Gosset,¹⁷ Y. Goto,^{60,61} R. Granier de Cassagnac,³⁹ N. Grau,^{3,15} S. V. Greene,⁷² G. Grim,⁴² M. Grosse Perdekamp,^{28,61} Y. Gu,⁶⁶ T. Gunji,¹³ L. Guo,⁴² H. Guragain,²³ H.-Å. Gustafsson,^{44,*} T. Hachiya,⁶⁰ A. Hadj Henni,⁶⁸ J. S. Haggerty,⁸ K. I. Hahn,²⁰ H. Hamagaki,¹³ J. Hamblen,⁶⁹ R. Han,⁵⁸ S. Y. Han,²⁰ J. Hanks,^{15,67} C. Harper,⁴⁹ E. P. Hartouni,⁴¹ K. Haruna,²⁵ S. Hasegawa,³² K. Hashimoto,^{60,62} E. Haslum,⁴⁴ R. Hayano,¹³ X. He,²³ M. Heffner,⁴¹ T. K. Hemmick,⁶⁷ T. Hester,⁹ J. C. Hill,³¹ M. Hohlmann,²¹ R. S. Hollis,⁹ W. Holzmann,^{15,66} K. Homma,²⁵ B. Hong,³⁶ T. Horaguchi,^{13,25,60,71} Y. Hori,¹³ D. Hornback,^{56,69} T. Hoshino,²⁵ J. Huang,⁸ S. Huang,⁷² T. Ichihara,^{60,61} R. Ichimiya,⁶⁰ H. Inuma,^{35,38,60} Y. Ikeda,^{60,71} K. Imai,^{32,38,60} Y. Imazu,⁶⁰ J. Imrek,¹⁸ M. Inaba,⁷¹ A. Iordanova,⁹ D. Isenhower,¹ M. Ishihara,⁶⁰ T. Isobe,^{13,60} M. Issah,^{66,72} A. Isupov,³³ D. Ivanischev,⁵⁹ D. Ivanischev,⁵⁹ Y. Iwanaga,²⁵ B. V. Jacak,⁶⁷ S. J. Jeon,⁵⁰ M. Jezghani,²³ J. Jia,^{8,15,66} X. Jiang,⁴² J. Jin,¹⁵ D. John,⁶⁹ B. M. Johnson,⁸ T. Jones,¹ E. Joo,³⁶ K. S. Joo,⁵⁰ D. Jouan,⁵⁷ D. S. Jumper,^{1,28} F. Kajihara,¹³ S. Kametani,⁶⁰ N. Kamihara,⁶¹ J. Kamin,⁶⁷ S. Kaneti,⁶⁷ B. H. Kang,²⁴ J. H. Kang,⁷⁶ J. S. Kang,²⁴ J. Kapustinsky,⁴² K. Karatsu,^{38,60} M. Kasai,^{60,62} D. Kawai,^{46,61} M. Kawashima,^{60,62} A. V. Kazantsev,³⁷ T. Kempel,³¹ J. A. Key,⁵³ V. Khachatryan,⁶⁷ A. Khanzadeev,⁵⁹ K. Kihara,⁷¹ K. M. Kijima,²⁵ J. Kikuchi,⁷³ A. Kim,²⁰ B. I. Kim,³⁶ C. Kim,³⁶ D. H. Kim,^{20,50} D. J. Kim,^{34,76} E. Kim,⁶⁵ E.-J. Kim,¹¹ H.-J. Kim,⁷⁶ M. Kim,⁶⁵ S. H. Kim,⁷⁶ Y.-J. Kim,²⁸ Y. K. Kim,²⁴ E. Kinney,¹⁴ K. Kiriluk,¹⁴ Á. Kiss,¹⁹ E. Kistenev,⁸ J. Klatsky,²² J. Klay,⁴¹ C. Klein-Boesing,⁴⁸ D. Kleinjan,⁹ P. Kline,⁶⁷ T. Koblesky,¹⁴ L. Kochenda,⁵⁹ M. Kofarago,¹⁹ B. Komkov,⁵⁹ M. Konno,⁷¹ J. Koster,^{28,61} D. Kotov,^{59,63} A. Kozlov,⁷⁴ A. Král,¹⁶ A. Kravitz,¹⁵ G. J. Kunde,⁴² K. Kurita,^{60,62} M. Kurosawa,^{60,61} M. J. Kweon,³⁶ Y. Kwon,^{69,76} G. S. Kyle,⁵⁴ R. Lacey,⁶⁶ Y. S. Lai,¹⁵ J. G. Lajoie,³¹ D. Layton,²⁸ A. Lebedev,³¹ D. M. Lee,⁴² J. Lee,²⁰ K. B. Lee,^{36,42} K. S. Lee,³⁶ S. H. Lee,⁶⁷ S. R. Lee,¹¹ T. Lee,⁶⁵ M. J. Leitch,⁴² M. A. L. Leite,⁶⁴ M. Leitgab,²⁸ B. Lenzi,⁶⁴ X. Li,¹² P. Lichtenwalner,⁴⁹ P. Liebing,⁶¹ S. H. Lim,⁷⁶ L. A. Linden Levy,¹⁴ T. Liška,¹⁶ A. Litvinenko,³³ H. Liu,^{42,54} M. X. Liu,⁴² B. Love,⁷² D. Lynch,⁸ C. F. Maguire,⁷² Y. I. Makdisi,⁷ M. Makek,^{74,77} A. Malakhov,³³ M. D. Malik,⁵³ A. Manion,⁶⁷ V. I. Manko,³⁷ E. Mannel,^{8,15} Y. Mao,^{58,60} L. Mašek,^{10,30} H. Masui,⁷¹ F. Matathias,¹⁵ M. McCumber,^{14,42,67} P. L. McGaughey,⁴² D. McGlinchey,^{14,22} C. McKinney,²⁸ N. Means,⁶⁷ A. Meles,⁵⁴ M. Mendoza,⁹ B. Meredith,^{15,28} Y. Miake,⁷¹ T. Mibe,³⁵ A. C. Mignerey,⁴⁵ P. Mikeš,³⁰ K. Miki,^{60,71} A. J. Miller,¹ A. Milov,^{8,74} D. K. Mishra,⁵ M. Mishra,⁴ J. T. Mitchell,⁸ Y. Miyachi,^{60,70} S. Miyasaka,^{60,70} S. Mizuno,^{60,71} A. K. Mohanty,⁵ P. Montuenga,²⁸ H. J. Moon,⁵⁰ T. Moon,⁷⁶ Y. Morino,¹³ A. Morreale,⁹ D. P. Morrison,^{8,†} S. Motschwiller,⁴⁹ T. V. Moukhanova,³⁷ D. Mukhopadhyay,⁷² T. Murakami,^{38,60} J. Murata,^{60,62} A. Mwai,⁶⁶ S. Nagamiya,^{35,60} J. L. Nagle,^{14,‡} M. Naglis,⁷⁴ M. I. Nagy,^{19,75} I. Nakagawa,^{60,61} H. Nakagomi,^{60,71} Y. Nakamiya,²⁵ K. R. Nakamura,^{38,60} T. Nakamura,^{25,60} K. Nakano,^{60,70} S. Nam,²⁰ C. Natrass,⁶⁹ P. K. Netrakanti,⁵ J. Newby,⁴¹ M. Nguyen,⁶⁷ M. Nishida,^{25,60} T. Niida,⁷¹ R. Nouicer,^{8,61} N. Novitzky,³⁴ A. S. Nyanin,³⁷ C. Oakley,²³ E. O'Brien,⁸ S. X. Oda,¹³ C. A. Ogilvie,³¹ M. Oka,⁷¹ K. Okada,⁶¹ Y. Onuki,⁶⁰ J. D. Orjuela Koop,¹⁴ A. Oskarsson,⁴⁴ M. Ouchida,^{25,60} H. Ozaki,⁷¹ K. Ozawa,^{13,35} R. Pak,⁸ A. P. T. Palounek,⁴² V. Pantuev,^{29,67} V. Papavassiliou,⁵⁴ B. H. Park,²⁴ I. H. Park,²⁰ J. Park,⁶⁵ S. Park,⁶⁵ S. K. Park,³⁶ W. J. Park,³⁶ S. F. Pate,⁵⁴ L. Patel,²³ M. Patel,³¹ H. Pei,³¹ J.-C. Peng,²⁸ H. Pereira,¹⁷ D. V. Perepelitsa,^{8,15} G. D. N. Perera,⁵⁴ V. Peresedov,³³ D. Yu. Peressounko,³⁷ J. Perry,³¹ R. Petti,^{8,67} C. Pinkenburg,⁸ R. Pinson,¹ R. P. Pisani,⁸ M. Proissl,⁶⁷ M. L. Purschke,⁸ A. K. Purwar,⁴² H. Qu,²³ J. Rak,^{34,53} A. Rakotozafindrabe,³⁹ I. Ravinovich,⁷⁴ K. F. Read,^{56,69} S. Rembeczki,²¹ K. Reygers,⁴⁸ D. Reynolds,⁶⁶ V. Riabov,^{52,59} Y. Riabov,^{59,63} E. Richardson,⁴⁵ N. Riveli,⁵⁵ D. Roach,⁷² G. Roche,^{43,*} S. D. Rolnick,⁹ M. Rosati,³¹ C. A. Rosen,¹⁴ S. S. E. Rosendahl,⁴⁴ P. Rosnet,⁴³ Z. Rowan,⁶ J. G. Rubin,⁴⁷ P. Rukoyatkin,³³ P. Ružička,³⁰ V. L. Rykov,⁶⁰ B. Sahlmueller,^{48,67} N. Saito,^{35,38,60,61} T. Sakaguchi,⁸ S. Sakai,⁷¹ K. Sakashita,^{60,70} H. Sako,³² V. Samsonov,^{52,59}

S. Sano,^{13,73} M. Sarsour,²³ S. Sato,³² T. Sato,⁷¹ M. Savastio,⁶⁷ S. Sawada,³⁵ B. Schaefer,⁷² B. K. Schmoll,⁶⁹ K. Sedgwick,⁹ J. Seele,^{14,61} R. Seidl,^{28,60,61} A. Yu. Semenov,³¹ V. Semenov,^{27,29} A. Sen,⁶⁹ R. Seto,⁹ P. Sett,⁵ A. Sexton,⁴⁵ D. Sharma,^{67,74} I. Shein,²⁷ T.-A. Shibata,^{60,70} K. Shigaki,²⁵ H. H. Shim,³⁶ M. Shimomura,^{31,71} K. Shoji,^{38,60} P. Shukla,⁵ A. Sickles,⁸ C. L. Silva,^{31,42,64} D. Silvermyr,^{44,56} C. Silvestre,¹⁷ K. S. Sim,³⁶ B. K. Singh,⁴ C. P. Singh,⁴ V. Singh,⁴ M. Slunečka,¹⁰ T. Sodre,⁴⁹ A. Soldatov,²⁷ R. A. Soltz,⁴¹ W. E. Sondheim,⁴² S. P. Sorensen,⁶⁹ I. V. Sourikova,⁸ F. Staley,¹⁷ P. W. Stankus,⁵⁶ E. Stenlund,⁴⁴ M. Stepanov,^{46,54} A. Ster,⁷⁵ S. P. Stoll,⁸ T. Sugitate,²⁵ C. Suire,⁵⁷ A. Sukhanov,⁸ T. Sumita,⁶⁰ J. Sun,⁶⁷ J. Sziklai,⁷⁵ E. M. Takagui,⁶⁴ A. Takahara,¹³ A. Taketani,^{60,61} R. Tanabe,⁷¹ Y. Tanaka,⁵¹ S. Taneja,⁶⁷ K. Tanida,^{38,60,61,65} M. J. Tannenbaum,⁸ S. Tarafdar,^{4,74} A. Taranenko,^{52,66} P. Tarján,¹⁸ E. Tennant,⁵⁴ H. Themann,⁶⁷ D. Thomas,¹ T. L. Thomas,⁵³ A. Timilsina,³¹ T. Todoroki,^{60,71} M. Togawa,^{38,60,61} A. Toia,⁶⁷ L. Tomášek,³⁰ M. Tomášek,^{16,30} Y. Tomita,⁷¹ H. Torii,^{13,25,60} M. Towell,¹ R. Towell,¹ R. S. Towell,¹ V.-N. Tram,³⁹ I. Tserruya,⁷⁴ Y. Tsuchimoto,²⁵ K. Utsunomiya,¹³ C. Vale,^{8,31} H. Valle,⁷² H. W. van Hecke,⁴² M. Vargyas,⁷⁵ E. Vazquez-Zambrano,¹⁵ A. Veicht,^{15,28} J. Velkovska,⁷² R. Vértesi,^{18,75} A. A. Vinogradov,³⁷ M. Virius,¹⁶ A. Vossen,²⁸ V. Vrba,^{16,30} E. Vznuzdaev,⁵⁹ X. R. Wang,⁵⁴ D. Watanabe,²⁵ K. Watanabe,⁷¹ Y. Watanabe,^{60,61} Y. S. Watanabe,^{13,35} F. Wei,^{31,54} R. Wei,⁶⁶ J. Wessels,⁴⁸ S. Whitaker,³¹ S. N. White,⁸ D. Winter,¹⁵ S. Wolin,²⁸ C. L. Woody,⁸ R. M. Wright,¹ M. Wysocki,^{14,56} B. Xia,⁵⁵ W. Xie,⁶¹ L. Xue,²³ S. Yalcin,⁶⁷ Y. L. Yamaguchi,^{13,60,73} K. Yamaura,²⁵ R. Yang,²⁸ A. Yanovich,²⁷ J. Ying,²³ S. Yokkaichi,^{60,61} J. S. Yoo,²⁰ I. Yoon,⁶⁵ Z. You,^{42,58} G. R. Young,⁵⁶ I. Younus,^{40,53} I. E. Yushmanov,³⁷ W. A. Zajc,¹⁵ O. Zaudtke,⁴⁸ A. Zelenski,⁷ C. Zhang,⁵⁶ S. Zhou,¹² and L. Zolin³³

(PHENIX Collaboration)

¹Abilene Christian University, Abilene, Texas 79699, USA

²Institute of Physics, Academia Sinica, Taipei 11529, Taiwan

³Department of Physics, Augustana College, Sioux Falls, South Dakota 57197, USA

⁴Department of Physics, Banaras Hindu University, Varanasi 221005, India

⁵Bhabha Atomic Research Centre, Bombay 400 085, India

⁶Baruch College, City University of New York, New York, New York 10010, USA

⁷Collider-Accelerator Department, Brookhaven National Laboratory, Upton, New York 11973-5000, USA

⁸Physics Department, Brookhaven National Laboratory, Upton, New York 11973-5000, USA

⁹University of California-Riverside, Riverside, California 92521, USA

¹⁰Charles University, Ovocný trh 5, Praha 1, 116 36 Prague, Czech Republic

¹¹Chonbuk National University, Jeonju 561-756, Korea

¹²Science and Technology on Nuclear Data Laboratory, China Institute of Atomic Energy, Beijing 102413, People's Republic of China

¹³Center for Nuclear Study, Graduate School of Science, University of Tokyo, 7-3-1 Hongo, Bunkyo, Tokyo 113-0033, Japan

¹⁴University of Colorado, Boulder, Colorado 80309, USA

¹⁵Columbia University, New York, New York 10027, USA and Nevis Laboratories, Irvington, New York 10533, USA

¹⁶Czech Technical University, Zikova 4, 166 36 Prague 6, Czech Republic

¹⁷Dapnia, CEA Saclay, F-91191 Gif-sur-Yvette, France

¹⁸Debrecen University, Egyetem tér 1, H-4010 Debrecen, Hungary

¹⁹ELTE, Eötvös Loránd University, Pázmány Péter sétány 1/A, H-1117 Budapest, Hungary

²⁰Ewha Womans University, Seoul 120-750, Korea

²¹Florida Institute of Technology, Melbourne, Florida 32901, USA

²²Florida State University, Tallahassee, Florida 32306, USA

²³Georgia State University, Atlanta, Georgia 30303, USA

²⁴Hanyang University, Seoul 133-792, Korea

²⁵Hiroshima University, Kagamiyama, Higashi-Hiroshima 739-8526, Japan

²⁶Department of Physics and Astronomy, Howard University, Washington, DC 20059, USA

²⁷IHEP Protvino, State Research Center of Russian Federation, Institute for High Energy Physics, Protvino 142281, Russia

²⁸University of Illinois at Urbana-Champaign, Urbana, Illinois 61801, USA

²⁹Institute for Nuclear Research of the Russian Academy of Sciences, prospekt 60-letiya Oktyabrya 7a, Moscow 117312, Russia

³⁰Institute of Physics, Academy of Sciences of the Czech Republic, Na Slovance 2, 182 21 Prague 8, Czech Republic

³¹Iowa State University, Ames, Iowa 50011, USA

³²Advanced Science Research Center, Japan Atomic Energy Agency, 2-4 Shirakata Shirane, Tokai-mura, Naka-gun, Ibaraki-ken 319-1195, Japan

³³Joint Institute for Nuclear Research, 141980 Dubna, Moscow Region, Russia

³⁴Helsinki Institute of Physics and University of Jyväskylä, P.O. Box 35, FI-40014 Jyväskylä, Finland

³⁵KEK, High Energy Accelerator Research Organization, Tsukuba, Ibaraki 305-0801, Japan

³⁶Korea University, Seoul 136-701, Korea

³⁷Russian Research Center "Kurchatov Institute," Moscow 123098, Russia

³⁸Kyoto University, Kyoto 606-8502, Japan

³⁹Laboratoire Leprince-Ringuet, Ecole Polytechnique, CNRS-IN2P3, Route de Saclay, F-91128 Palaiseau, France

⁴⁰Physics Department, Lahore University of Management Sciences, Lahore 54792, Pakistan

⁴¹Lawrence Livermore National Laboratory, Livermore, California 94550, USA

⁴²Los Alamos National Laboratory, Los Alamos, New Mexico 87545, USA

⁴³LPC, Université Blaise Pascal, CNRS-IN2P3, Clermont-Fd, 63177 Aubiere Cedex, France

⁴⁴Department of Physics, Lund University, Box 118, SE-221 00 Lund, Sweden

⁴⁵University of Maryland, College Park, Maryland 20742, USA

⁴⁶Department of Physics, University of Massachusetts, Amherst, Massachusetts 01003-9337, USA

⁴⁷Department of Physics, University of Michigan, Ann Arbor, Michigan 48109-1040, USA

⁴⁸Institut für Kernphysik, University of Muenster, D-48149 Muenster, Germany

⁴⁹Muhlenberg College, Allentown, Pennsylvania 18104-5586, USA

⁵⁰Myongji University, Yongin, Kyonggido 449-728, Korea

⁵¹Nagasaki Institute of Applied Science, Nagasaki-shi, Nagasaki 851-0193, Japan

⁵²National Research Nuclear University, MEPHI, Moscow Engineering Physics Institute, Moscow 115409, Russia

⁵³University of New Mexico, Albuquerque, New Mexico 87131, USA

⁵⁴New Mexico State University, Las Cruces, New Mexico 88003, USA

⁵⁵Department of Physics and Astronomy, Ohio University, Athens, Ohio 45701, USA

⁵⁶Oak Ridge National Laboratory, Oak Ridge, Tennessee 37831, USA

⁵⁷IPN-Orsay, Université Paris Sud, CNRS-IN2P3, BP1, F-91406 Orsay, France

⁵⁸Peking University, Beijing 100871, People's Republic of China

⁵⁹PNPI, Petersburg Nuclear Physics Institute, Gatchina, Leningrad Region 188300, Russia

⁶⁰RIKEN Nishina Center for Accelerator-Based Science, Wako, Saitama 351-0198, Japan

⁶¹RIKEN BNL Research Center, Brookhaven National Laboratory, Upton, New York 11973-5000, USA

⁶²Physics Department, Rikkyo University, 3-34-1 Nishi-Ikebukuro, Toshima, Tokyo 171-8501, Japan

⁶³Saint Petersburg State Polytechnic University, St. Petersburg 195251, Russia

⁶⁴Universidade de São Paulo, Instituto de Física, Caixa Postal 66318, São Paulo CEP05315-970, Brazil

⁶⁵Department of Physics and Astronomy, Seoul National University, Seoul 151-742, Korea

⁶⁶Chemistry Department, Stony Brook University, SUNY, Stony Brook, New York 11794-3400, USA

⁶⁷Department of Physics and Astronomy, Stony Brook University, SUNY, Stony Brook, New York 11794-3800, USA

⁶⁸SUBATECH (Ecole des Mines de Nantes, CNRS-IN2P3, Université de Nantes) BP 20722, 44307 Nantes, France

⁶⁹University of Tennessee, Knoxville, Tennessee 37996, USA

⁷⁰Department of Physics, Tokyo Institute of Technology, Oh-okayama, Meguro, Tokyo 152-8551, Japan

⁷¹Institute of Physics, University of Tsukuba, Tsukuba, Ibaraki 305, Japan

⁷²Vanderbilt University, Nashville, Tennessee 37235, USA

⁷³Waseda University, Advanced Research Institute for Science and Engineering, 17 Kikui-cho, Shinjuku-ku, Tokyo 162-0044, Japan

⁷⁴Weizmann Institute, Rehovot 76100, Israel

⁷⁵Institute for Particle and Nuclear Physics, Wigner Research Centre for Physics, Hungarian Academy of Sciences (Wigner RCP, RMKI),

PO Box 49, H-1525 Budapest 114, Hungary

⁷⁶Yonsei University, IPAP, Seoul 120-749, Korea

⁷⁷University of Zagreb, Faculty of Science, Department of Physics, Bijenička 32, HR-10002 Zagreb, Croatia

(Received 18 November 2014; published 10 March 2015)

The standard model (SM) of particle physics is spectacularly successful, yet the measured value of the muon anomalous magnetic moment $(g - 2)_\mu$ deviates from SM calculations by 3.6σ . Several theoretical models attribute this to the existence of a “dark photon,” an additional U(1) gauge boson, which is weakly coupled to ordinary photons. The PHENIX experiment at the Relativistic Heavy Ion Collider has searched for a dark photon, U , in $\pi^0, \eta \rightarrow \gamma e^+ e^-$ decays and obtained upper limits of $\mathcal{O}(2 \times 10^{-6})$ on U - γ mixing at 90% C.L. for the mass range $30 < m_U < 90 \text{ MeV}/c^2$. Combined with other experimental limits, the remaining region in the U - γ mixing parameter space that can explain the $(g - 2)_\mu$ deviation from its SM value is nearly completely excluded at the 90% confidence level, with only a small region of $29 < m_U < 32 \text{ MeV}/c^2$ remaining.

DOI: 10.1103/PhysRevC.91.031901

PACS number(s): 25.75.Dw

Introduction. The standard model (SM) of particle physics provides unprecedented numerical accuracy for quantities such

as the anomalous magnetic moment of the electron $(g - 2)_e$ and predicts the existence of the vector bosons W^\pm and Z^0 and the recently discovered Higgs boson. Hence, measurements that lie outside SM predictions warrant special scrutiny. One such result is the measured value of $(g - 2)_\mu$ for the muon [1], which deviates from SM calculations by 3.6σ [2]. An intriguing explanation for this discrepancy has been proposed by adding a “dark” gauge boson [3–6]. While the possibility

*Deceased.

[†]PHENIX cospokesperson: morrison@bnl.gov

[‡]PHENIX cospokesperson: jamie.nagle@colorado.edu

of a hidden U(1) gauge sector had been considered shortly after the advent of the SM [7,8], it has recently gained more relevance, because it provides a simultaneous explanation of various beyond-the-SM phenomena in addition to $(g-2)_\mu$. These include, for example, the discrepancy between the world's data on proton charge radius [9] and that obtained by the Lamb shift in muonic hydrogen [10,11] and the positron excess in cosmic rays observed by ATIC [12], PAMELA [13], and AMS-II [14] by providing a new mechanism for the decay of dark matter [15,16].

While a variety of mechanisms can be introduced to parametrize dark-sector physics, a simple formulation postulates a “dark photon” of mass m_U that mixes with QED photons via a “kinetic coupling” term in the Lagrangian [7,8,17,18]

$$\mathcal{L}_{\text{mix}} = -\frac{\varepsilon}{2} F_{\mu\nu}^{\text{QED}} F_{\text{dark}}^{\mu\nu}, \quad (1)$$

where ε parametrizes the mixing strength. Dark photons can then mix with QED photons through all processes that involve QED photons, with an effective strength $\alpha_U = \varepsilon^2 \alpha_{EM}$. If the dark photon mass exceeds twice the electron mass, it can decay into an e^+e^- pair, and in the minimal version of the model; this is its dominant decay mode in the interval $2m_e < m_U < 2m_\mu$. To date, a wide range of searches [18] has excluded most of the $[m_U, \varepsilon]$ parameter space that could explain the deviation of $(g-2)_\mu$ from its SM value. In this work, we report on new limits that exclude at the 90% confidence level essentially all of the remaining allowed parameter space, thereby rendering the dark photon an unlikely candidate to resolve the discrepancy of $(g-2)_\mu$ with the SM.

Searching for $\pi^0, \eta \rightarrow \gamma U, U \rightarrow e^+e^-$. We search for possible decays of $\pi^0, \eta \rightarrow \gamma U, U \rightarrow e^+e^-$ by examining the invariant mass m_{ee} of e^+e^- pairs in a large sample of Dalitz decays, $\pi^0, \eta \rightarrow \gamma e^+e^-$ for $30 < m_U < 90 \text{ MeV}/c^2$ in the dark photon parameter space, where the possibility of disentangling the $(g-2)_\mu$ anomaly by the dark photon survives at the 90% confidence level. The invariant yield of virtual photons from the Dalitz decays of π^0, η is given by the Kroll-Wada equation [19],

$$\left(\frac{dN_{ee}}{dm_{ee}}\right)_{\gamma e^+e^-} = N_{2\gamma} \frac{4\alpha_{EM}}{3\pi} \frac{1}{m_{ee}} K W_{\pi^0, \eta}(m_{ee}) |F(m_{ee}^2)|^2, \quad (2)$$

where

$$K W_{\pi^0, \eta}(m_{ee}) = \sqrt{1 - \frac{4m_e^2}{m_{ee}^2}} \left(1 + \frac{2m_e^2}{m_{ee}^2}\right) \left(1 - \frac{m_{ee}^2}{m_{\pi^0, \eta}^2}\right)^3, \quad (3)$$

$N_{2\gamma}$ is the invariant yield of 2γ decays of π^0, η , α_{EM} is the fine structure constant, and $m_e, m_{\pi^0, \eta}$ are masses for the electron, π^0 and η , respectively. The deviation of the transition form factor $F(q^2)$ from unity is 0.0157 even at $m_{ee} = 90 \text{ MeV}/c^2$ from the parametrization of $F(q^2) = (1 - q^2/\Lambda^2)^{-1}$ with $\Lambda = 0.72 \text{ GeV}$ [20]. Therefore, the variation of $F(q^2)$ is small enough in the mass range of interest to set $F(q^2) = 1$ in the calculation. The weak coupling of the dark photon to the QED photon implies that the natural width of the dark photon is very narrow, and as a result the expected line shape of the dark

photon is set by the mass resolution, σ , of the detector,

$$\left(\frac{dN_{ee}}{dm_{ee}}\right)_{\gamma U} = N_{2\gamma} \frac{2\varepsilon^2}{\sqrt{2\pi}\sigma} e^{-\frac{(m_{ee}-m_U)^2}{2\sigma^2}} K W_{\pi^0, \eta}(m_{ee}). \quad (4)$$

From the peak-height ratio,

$$R(m_U) = (dN_{ee}/dm_{ee})_{\pi^0, \eta \rightarrow \gamma U} / (dN_{ee}/dm_{ee})_{\pi^0, \eta \rightarrow \gamma e^+e^-}, \quad (5)$$

the dark photon mixing parameter can then be determined as

$$\varepsilon^2 = \frac{2\alpha_{EM}}{3\pi} \frac{\sigma}{m_U} \sqrt{2\pi} R(m_U). \quad (6)$$

Note that in this approach the efficiencies for detection of e^+e^- pairs from Dalitz decays and from dark photons cancel in the ratio $R(m_U)$.

The analysis presented here is based on a precise measurement of virtual photons from π^0 and η Dalitz decays [21] across three PHENIX data sets at a collision energy of $\sqrt{s_{NN}} = 200 \text{ GeV}$ with an integrated luminosity of 4.8 pb^{-1} of $p + p$ collected in 2006, 82.3 nb^{-1} of $d + \text{Au}$ collected in 2008, and 6.0 pb^{-1} of $p + p$ collected in 2009. Here the $d + \text{Au}$ statistics corresponds to $2 \times 197 \times 82.3 \text{ nb}^{-1} = 32.4 \text{ pb}^{-1}$ of nucleon-nucleon collisions. All three data sets include an electron triggered sample, and the single electron trigger threshold for the $d + \text{Au}$ run was higher than that for the $p + p$ runs. A hadron blind detector (HBD) [22] was installed in the experiment around the primary collision point prior to the 2009 data taking period. The additional material of the HBD resulted in a corresponding increase in the external photon conversion rate. The experiment was also operated with a reduced magnetic field integral during the period of HBD data taking. These effects substantially alter the shape of the 2009 e^+e^- mass spectrum below $35 \text{ MeV}/c^2$ relative to the spectra from 2006 and 2008. Therefore, we restrict the 2009 analysis to the mass region above $40 \text{ MeV}/c^2$ to avoid the edge effect at parametrization of the Dalitz contribution.

The PHENIX apparatus [23] was designed with only 0.39% of a radiation length (X_0) in front of the tracking detectors. It generates a small rate of conversions in the experimental aperture and provides excellent momentum resolution and electron identification. The HBD brought an additional material budget of $2.4\% \times X_0$ for the 2009 run. The tracking system comprises drift wire and pad chambers with a momentum resolution of $\delta p/p = 1\% \oplus 1.1\% \times p$ [GeV/c]. Charged tracks with momenta above 0.2 GeV/c and pseudorapidity $|\eta| < 0.35$ fall within the PHENIX acceptance. Electron identification requires hits in a Ring Imaging Čerenkov detector and energy-momentum matching in an electromagnetic calorimeter with an energy resolution of $\delta E/E < 10\%/\sqrt{E[\text{GeV}]}$.

All combinations of electrons and positrons in an event are taken as pairs for the analysis. The contributions owing to random combinations, correlated fake pairs from double Dalitz decays ($\pi^0, \eta \rightarrow e^+e^-e^+e^-$), and jet-induced correlations are evaluated using like-sign pairs. After scaling by the number of nucleon-nucleon collisions, the correlated backgrounds in $p + p$ and $d + \text{Au}$ are very similar, indicating that these background contributions are well understood. Pairs stemming from photon conversions in the material of the detector are

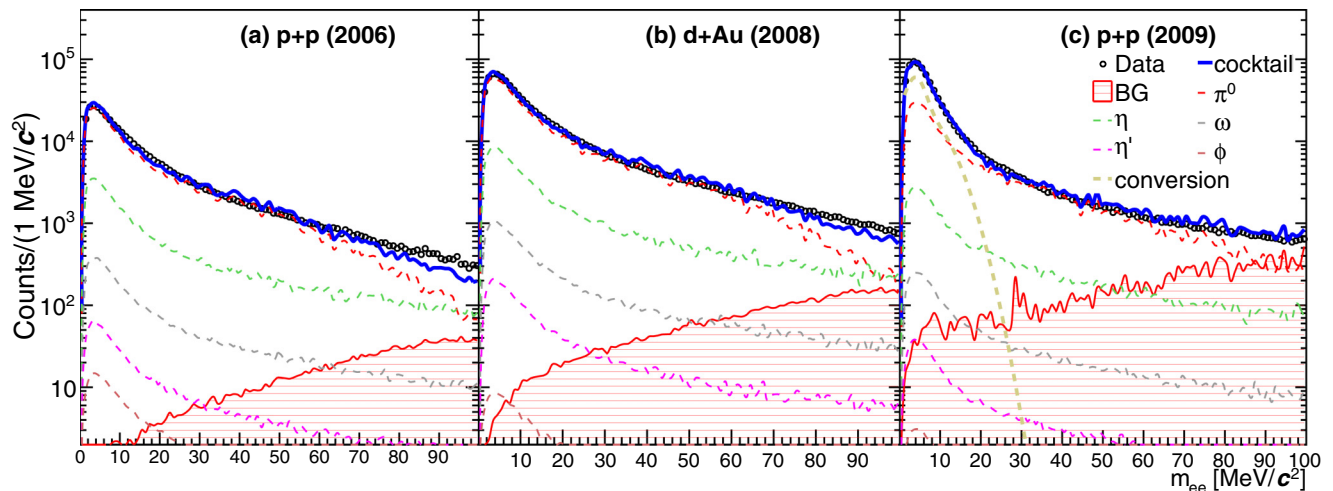


FIG. 1. (Color online) The raw spectra of e^+e^- pairs for the 2006 $p + p$, 2008 $d + Au$, and 2009 $p + p$ data sets. The contributions of various background components to the measured invariant mass spectra are shown. The 2009 $p + p$ data have a significant contribution to the conversion background coming from the material of the HBD that is not present in the 2006 and 2008 data sets.

removed by a cut on their characteristic angular orientation with respect to the magnetic field [24]. For the 2009 $p + p$ data, conversion pairs are rejected by a cut on the cluster size in the HBD, which depends on the pair opening angle [25], because the lower magnetic field of the 2009 run reduces the rejection power of the angular orientation cut. Conversions in the HBD readout plane were removed by an analysis technique of mass reconstruction assuming electrons come from the HBD readout plane [26]. In the 2009 data set we consider pairs with an invariant mass above $40 \text{ MeV}/c^2$, where the contribution of conversion pairs becomes negligible. Excluding these nonhadronic background pairs, we obtained 67 000, 167 000, and 75 000 e^+e^- pairs for 2006 $p + p$, 2008 $d + Au$, and 2009 $p + p$, respectively, in the mass range $30 < m_{ee} < 90 \text{ MeV}/c^2$, where most pairs originate from π^0, η Dalitz decays. Contributions to the electron pair spectrum are estimated by a GEANT3-based detector simulation using the measured invariant yields for hadrons as input. Effects such as the single electron trigger efficiency and inactive areas in the detector are taken into account. Figure 1 shows the raw spectra of e^+e^- pairs with the hadronic decay and background contributions for the 2006 $p + p$, 2008 $d + Au$, and 2009 $p + p$ data sets.

If the expected dark photon invariant mass distribution follows a normal distribution, then the standard deviation is equal to the detector mass resolution, as already described. This resolution is determined using a Monte Carlo procedure based on a GEANT3 description of the experimental apparatus. Spectra of dark photons with a flat distribution in transverse momentum for $p_T < 5 \text{ GeV}/c$, covering the full azimuth, with rapidity $|y| < 0.5$, and with an initial vertex within 35 cm of the nominal vertex position are generated and forced to decay as $U \rightarrow e^+e^-$. Dark photon masses from 20–90 MeV/c^2 were investigated, with 20×10^6 decays generated at each mass hypothesis. The reconstructed e^+e^- pairs were then weighted according to their pair p_T to follow the experimental e^+e^- pair spectrum after background subtraction. The e^+e^- invariant mass resolution for the PHENIX detector in

$30 < m_{ee} < 90 \text{ MeV}/c^2$ is $\sigma = 3.1 \text{ MeV}/c^2$, with a 3% uncertainty. The calculated mass resolution is also confirmed with the data via a shape matching of the π^0 Dalitz peak around $5 \text{ MeV}/c^2$.

To establish a limit on the dark photon yield, we first describe the shape of the background-subtracted e^+e^- spectrum with a physics-motivated curve composed of the Kroll-Wada formula for virtual photon yield from both the π^0 and the η multiplied by a fourth-order Chebychev polynomial $T_4(x)$ to allow for slight deviations owing to various detector effects:

$$f(m_{ee}) = \frac{1}{m_{ee}} \times \left[\left(1 - \frac{m_{ee}^2}{m_{\pi^0}^2} \right)^3 + r_{\eta/\pi^0} \times \left(1 - \frac{m_{ee}^2}{m_{\eta}^2} \right)^3 \right] \times T_4(m_{ee}). \quad (7)$$

The η/π^0 ratio, r_{η/π^0} , is fixed at 0.17, a value determined using a realistic “cocktail” of hadronic decays filtered through a model of the detector acceptance. The ω/π^0 ratio is fixed at 0.03. The shapes of the e^+e^- mass spectra from η and ω decays are indistinguishable for $m_{ee} < 100 \text{ MeV}/c^2$, and their combined yield relative to the π^0 , $0.17 + 0.03 = 0.20$, is taken as the effective η/π^0 ratio for the analysis.

We divide the full mass ranges of $25 < m_{ee} < 95 \text{ MeV}/c^2$ and $35 < m_{ee} < 95 \text{ MeV}/c^2$ into lower and higher mass ranges after nonhadronic background subtraction, use Eq. (7) to describe each portion, and demand continuity of the model at the mass where the two ranges abut. A simultaneous fit to the three mass spectra, allowing each an independent normalization, results in a combined description of the Dalitz continuum. This procedure produces a lower reduced χ^2 for the overall fit than using a single mass range for each data set. The break point dividing the lower and upper mass ranges was allowed to vary, with $61 \text{ MeV}/c^2$ giving the best reduced χ^2 .

Figure 2 shows the best-fit result to the Dalitz decay contribution in each data set after subtraction of unphysical background pairs. The contribution of the fit procedure to the total uncertainty is explored by varying the break point above and below this preferred value until the reduced χ^2 statistic

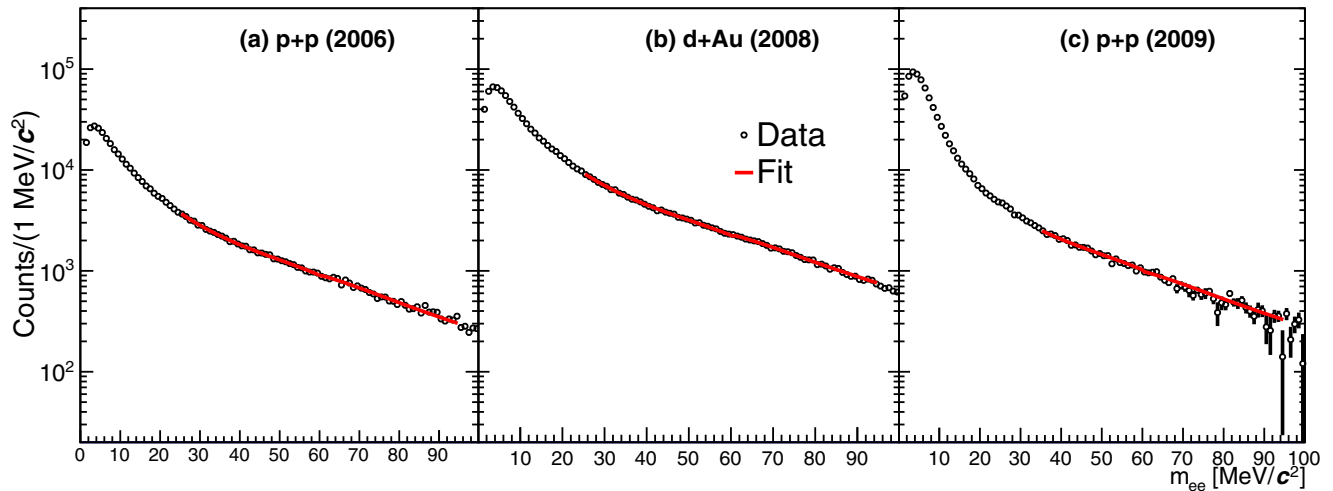


FIG. 2. (Color online) The best fit to the three mass spectra with the physics-motivated function describing the e^+e^- distributions from hadron decays.

risers by one and then taking the resulting 16% effect on the experimental sensitivity as the systematic uncertainty owing to the procedure.

Results. The fitted background describes the yield of e^+e^- counts absent a dark photon signal. We employ the C.L._s statistical approach [27] to determine a limit on the number of dark photon candidates, which is in line with the current practice of setting limits for a hypothetical particle. This method has the effect of reducing the strength of the limit determination in the case of low (or no) signal strength, generally resulting in a conservative estimate of the C.L. We step through the full mass range with a $1 \text{ MeV}/c^2$ step repeatedly refitting the spectrum with the addition of a Gaussian of width equal to the mass resolution and centered at each mass hypothesis. This determines the observed yield as a function of m_U , which may be greater or less than the experimental sensitivity at each mass, with a significance that is determined by the underlying probability distribution of the background, which is calculated by a likelihood ratio between the signal + background and background-only hypotheses. The assumed background yield in any mass window will have uncertainties owing to statistical fluctuations in the data

used to determine the parameters describing the background by Eq. (7) and from systematic uncertainties in alternative background shapes. We evaluated the variation in the experimental sensitivity owing to fluctuations in these uncertainties in addition to the uncertainty in the e^+e^- mass resolution. The observed value, the experimental sensitivity, and one- and two-standard-deviation bands around the experimental sensitivity (shown as green and yellow bands) are all indicated on the plots for the different data sets as well as the combined result in Fig. 3.

The p value under the null hypothesis from the combined result is calculated considering only the statistical uncertainty and is always greater than 0.27 in the entire range $30 < m_U < 90 \text{ MeV}/c^2$. The minimum p value is consistent with the background-only hypothesis if the *look-elsewhere effect* [28] is taken into account. Therefore, the limit on the number of dark photon candidate events can be translated directly into a limit on the dark photon coupling parameter using the peak-height ratio, Eq. (5). Figure 4 shows the limit determined by PHENIX along with the 90% confidence level (C.L.) limits from the WASA [29], HADES [30], KLOE [31], A1(MAMI) [32], and BABAR [33] experiments and the 2σ

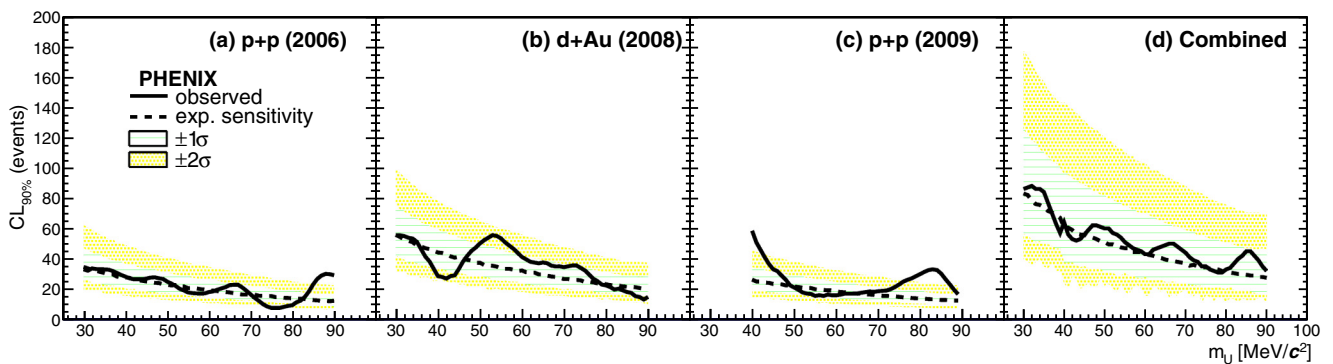


FIG. 3. (Color online) The experimental sensitivity and observed limit on the number of dark photon candidates as a function of the assumed dark photon mass. The $\pm 1\sigma$ and $\pm 2\sigma$ bands of the combined statistical and systematic uncertainties around the experimental sensitivity are shown in green and yellow, respectively.

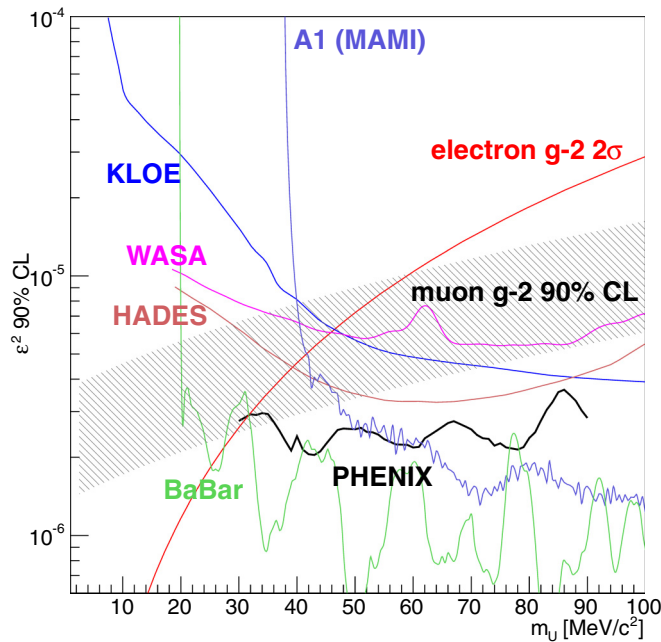


FIG. 4. (Color online) A compilation of the limits on the U - γ mixing parameter, showing the PHENIX results. Also shown are the limits at 90% C.L. from WASA [29], HADES [30], KLOE [31], A1(MAMI) [32], and BABAR [33] experiments and the band indicating the range of mass and coupling parameters favored by the $(g-2)_\mu$ anomaly at 90% C.L. Also shown is the 2σ upper limit obtained from $(g-2)_e$ [34].

upper limit theoretically calculated from $(g-2)_e$ [34]. The bands indicate the range of parameters that would allow the dark photon to explain the $(g-2)_\mu$ anomalies with the 90% C.L. The upward fluctuation apparent in the 2008 $d + Au$ data compensates for a downward fluctuation of similar scale in the 2009 $p + p$ data, leading to the slightly modulated limit of the combined result. The PHENIX results cover the mass range $30 < m_U < 90 \text{ MeV}/c^2$, and over that range set a stricter limit than those of WASA, HADES, or KLOE and complement the A1(MAMI) results for their less sensitive region below $50 \text{ MeV}/c^2$. The PHENIX limits exclude the values of the coupling favored by the $(g-2)_\mu$ anomaly above $m_U > 36 \text{ MeV}/c^2$. Recently, BABAR reported stricter limits from a search of the reaction $e^+e^- \rightarrow \gamma U, U \rightarrow l^+l^-$, excluding values of the preferred $(g-2)_\mu$ region for $m_U > 32 \text{ MeV}/c^2$, and covering a mass range up to $10.2 \text{ GeV}/c^2$. As a result, nearly all the available parameter space which would allow the dark photon to explain the $(g-2)_\mu$ results are ruled out at the 90% C.L. by independent experiments. Figure 5 shows the PHENIX limits in the dark photon parameter space with different confidence levels, focusing on the small remaining parameter space for $30 < m_U < 32 \text{ MeV}/c^2$. The entire parameter space to explain the $(g-2)_\mu$ anomaly by the dark photon can be excluded at the 85% C.L. by the PHENIX data alone. The level of the compatibility between our data and the coupling strength favored for the $(g-2)_\mu$ anomaly is 10% with a statistical test [35].

Conclusions. In summary, the PHENIX results set limits for the coupling of a dark photon to the QED photon over the mass

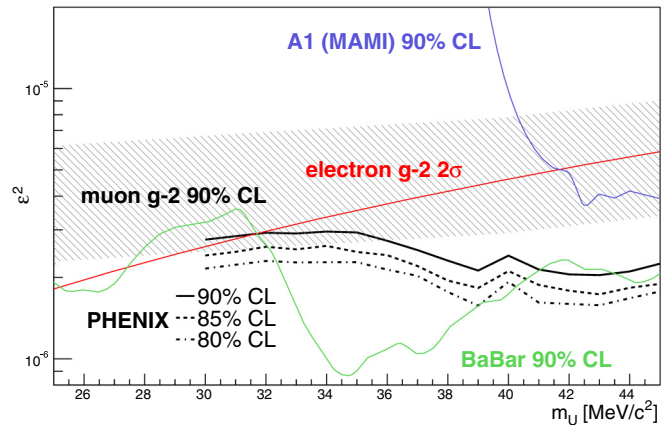


FIG. 5. (Color online) Limits on the U - γ mixing parameters from PHENIX at different confidence levels, together with the 90% C.L. limits from BABAR [33] and A1(MAMI) [32], the 2σ upper limit derived from $(g-2)_e$ [34], and the region favored by $(g-2)_\mu$.

range $30 < m_U < 90 \text{ MeV}/c^2$, improving upon the recent results of the KLOE, WASA, HADES, and A1 experiments. Combining with the BABAR results, the dark photon is ruled out at the 90% C.L. as an explanation for the $(g-2)_\mu$ anomaly for $m_U > 32 \text{ MeV}/c^2$, leaving only a small remaining part of parameter space in the region $29 < m_U < 32 \text{ MeV}/c^2$. The probability that the theoretically predicted coupling strength required to explain the $(g-2)_\mu$ anomaly is compatible with the PHENIX results is only 10%. Future analyses by PHENIX would be able to provide even more stringent limits owing to both increased data sets and improved detector technology that allow measurement of displaced vertices. As the coupling to the dark photon gets weaker, the distance traveled by the dark photon before decaying into e^+e^- grows longer [36]. The high-statistics data set taken after the recently commissioned PHENIX silicon vertex detector was installed in 2011 is being analyzed to look for such weakly coupled dark photons to provide limits even more restrictive than those reported here.

Acknowledgments. We thank the staff of the Collider-Accelerator and Physics Departments at Brookhaven National Laboratory and the staff of the other PHENIX participating institutions for their vital contributions. We also thank William Marciano and Hye-Sung Lee for useful discussions and theoretical calculations, and we thank the WASA, HADES, and BABAR collaborations for useful interactions. We acknowledge support from the Office of Nuclear Physics in the Office of Science of the Department of Energy, the National Science Foundation, a sponsored research grant from Renaissance Technologies LLC, Abilene Christian University Research Council, Research Foundation of SUNY, and Dean of the College of Arts and Sciences, Vanderbilt University (U.S.A.); Ministry of Education, Culture, Sports, Science, and Technology and the Japan Society for the Promotion of Science (Japan); Conselho Nacional de Desenvolvimento Científico e Tecnológico and Fundação de Amparo à Pesquisa do Estado de São Paulo (Brazil); Natural Science Foundation of China (People's Republic of China); Ministry of Science, Education, and Sports (Croatia); Ministry of Education, Youth

and Sports (Czech Republic); Centre National de la Recherche Scientifique, Commissariat à l'Énergie Atomique, and Institut National de Physique Nucléaire et de Physique des Particules (France); Bundesministerium für Bildung und Forschung, Deutscher Akademischer Austausch Dienst, and Alexander von Humboldt Stiftung (Germany); OTKA Grant No. NK 101 428 and the Ch. Simonyi Fund (Hungary); Department of Atomic Energy and Department of Science and Technology (India); Israel Science Foundation (Israel); Basic Science

Research Program through NRF of the Ministry of Education (Korea); Physics Department, Lahore University of Management Sciences (Pakistan); Ministry of Education and Science, Russian Academy of Sciences, Federal Agency of Atomic Energy (Russia); VR and Wallenberg Foundation (Sweden); the U.S. Civilian Research and Development Foundation for the Independent States of the Former Soviet Union; the Hungarian American Enterprise Scholarship Fund; and the U.S.-Israel Binational Science Foundation.

-
- [1] G. W. Bennett *et al.* (Muon G-2 Collaboration), Final report of the Muon E821 anomalous magnetic moment measurement at BNL, *Phys. Rev. D* **73**, 072003 (2006).
- [2] K. A. Olive *et al.* (Particle Data Group), Review of particle physics, *Chin. Phys. C* **38**, 090001 (2014).
- [3] P. Fayet, U-boson production in $e + e^-$ annihilations, psi and upsilon decays, and light dark matter, *Phys. Rev. D* **75**, 115017 (2007).
- [4] M. Pospelov, Secluded U(1) below the weak scale, *Phys. Rev. D* **80**, 095002 (2009).
- [5] M. Endo, K. Hamaguchi, and G. Mishima, Constraints on hidden photon models from electron g-2 and hydrogen spectroscopy, *Phys. Rev. D* **86**, 095029 (2012).
- [6] H. Davoudiasl, H.-S. Lee, and W. J. Marciano, Dark side of Higgs diphoton decays and Muon g-2, *Phys. Rev. D* **86**, 095009 (2012).
- [7] P. Galison and A. Manohar, Two Z's or not two Z's? *Phys. Lett. B* **136**, 279 (1984).
- [8] B. Holdom, Two U(1)'s and epsilon charge shifts, *Phys. Lett. B* **166**, 196 (1986).
- [9] P. J. Mohr, B. N. Taylor, and D. B. Newell, CODATA recommended values of the fundamental physical constants: 2006, *Rev. Mod. Phys.* **80**, 633 (2008).
- [10] R. Pohl *et al.*, The size of the proton, *Nature (London)* **466**, 213 (2010).
- [11] A. Antognini *et al.*, Proton structure from the measurement of 2S-2P transition frequencies of muonic hydrogen, *Science* **339**, 417 (2013).
- [12] J. Chang *et al.*, An excess of cosmic ray electrons at energies of 300-800 GeV, *Nature (London)* **456**, 362 (2008).
- [13] O. Adriani *et al.* (PAMELA Collaboration), An anomalous positron abundance in cosmic rays with energies 1.5-100 GeV, *Nature (London)* **458**, 607 (2009).
- [14] M. Aguilar *et al.* (AMS Collaboration), First result from the alpha magnetic spectrometer on the International Space Station: Precision measurement of the positron fraction in primary cosmic rays of 0.5-350 GeV, *Phys. Rev. Lett.* **110**, 141102 (2013).
- [15] N. Arkani-Hamed, D. P. Finkbeiner, T. R. Slatyer, and N. Weiner, A theory of dark matter, *Phys. Rev. D* **79**, 015014 (2009).
- [16] D. Tucker-Smith and I. Yavin, Muonic hydrogen and MeV forces, *Phys. Rev. D* **83**, 101702 (2011).
- [17] J. Jaeckel, A force beyond the standard model- status of the quest for hidden photons, *Frascati Phys. Ser.* **56**, 172 (2012).
- [18] R. Essig *et al.*, Dark sectors and new, light, weakly-coupled particles, [arXiv:1311.0029](https://arxiv.org/abs/1311.0029).
- [19] N. M. Kroll and W. Wada, Internal pair production associated with the emission of high-energy gamma rays, *Phys. Rev.* **98**, 1355 (1955).
- [20] R. I. Dzhelyadin *et al.* (SERPUKHOV-134 Collaboration), Investigation of η meson electromagnetic structure in $\eta \rightarrow \mu^+ \mu^- \gamma$ decay, *Phys. Lett. B* **94**, 548 (1980).
- [21] A. Adare *et al.* (PHENIX Collaboration), Direct photon production in $d + Au$ collisions at $\sqrt{s_{NN}} = 200$ GeV, *Phys. Rev. C* **87**, 054907 (2013).
- [22] W. Anderson *et al.* (PHENIX Collaboration), Design, construction, operation and performance of a hadron blind detector for the PHENIX experiment, *Nucl. Instrum. Methods Phys. Res., Sect. A* **646**, 35 (2011).
- [23] K. Adcox *et al.* (PHENIX Collaboration), PHENIX detector overview, *Nucl. Instrum. Methods Phys. Res., Sect. A* **499**, 469 (2003).
- [24] A. Adare *et al.* (PHENIX Collaboration), Detailed measurement of the e^+e^- pair continuum in $p + p$ and Au + Au collisions at $\sqrt{s_{NN}} = 200$ GeV and implications for direct photon production, *Phys. Rev. C* **81**, 034911 (2010).
- [25] A. Adare *et al.* (PHENIX Collaboration), Double spin asymmetry of electrons from heavy flavor decays in $p + p$ collisions at $\sqrt{s} = 200$ GeV, *Phys. Rev. D* **87**, 012011 (2013).
- [26] A. Adare *et al.* (PHENIX Collaboration), Centrality Dependence of Low-momentum Direct-photon Production in Au + Au Collisions at $\sqrt{s_{NN}} = 200$ GeV, [arXiv:1405.3940](https://arxiv.org/abs/1405.3940).
- [27] A. L. Read, Presentation of search results: The CL(s) technique, *J. Phys. G* **28**, 2693 (2002).
- [28] E. Gross and O. Vitells, Trial factors for the look elsewhere effect in high energy physics, *Eur. Phys. J. C* **70**, 525 (2010).
- [29] P. Adlarson *et al.* (WASA-at-COSY Collaboration), Search for a dark photon in the $\pi^0 \rightarrow e^+e^- \gamma$ decay, *Phys. Lett. B* **726**, 187 (2013).
- [30] G. Agakishiev *et al.* (HADES Collaboration), Searching a dark photon with HADES, *Phys. Lett. B* **731**, 265 (2014).
- [31] D. Babusci *et al.* (KLOE-2 Collaboration), Limit on the production of a light vector gauge boson in phi meson decays with the KLOE detector, *Phys. Lett. B* **720**, 111 (2013).
- [32] H. Merkel *et al.* (MAMI Collaboration), Search for light massive gauge bosons as an explanation of the $(g - 2)_\mu$ anomaly at MAMI, *Phys. Rev. Lett.* **112**, 221802 (2014).
- [33] J. P. Lees *et al.* (BABAR Collaboration), Search for a dark photon in e^+e^- collisions at BaBar, *Phys. Rev. Lett.* **113**, 201801 (2014).
- [34] H. Davoudiasl, H.-S. Lee, and W. J. Marciano, Muon g-2, rare kaon decays, and parity violation from dark bosons, *Phys. Rev. D* **89**, 095006 (2014).
- [35] M. Maltoni and T. Schwetz, Testing the statistical compatibility of independent data sets, *Phys. Rev. D* **68**, 033020 (2003).
- [36] J. D. Bjorken, R. Essig, P. Schuster, and N. Toro, New fixed-target experiments to search for dark gauge forces, *Phys. Rev. D* **80**, 075018 (2009).